Clim Dyn
DOI 10.1007/s00382-009-0531-x

Mechanisms of diurnal precipitation over the US Great Plains: a cloud resolving model perspective

Myong-In Lee · Ildae Choi · Wei-Kuo Tao · Siegfried D. Schubert · In-Sik Kang

Received: 5 August 2008 / Accepted: 20 January 2009

Abstract The mechanisms of summertime diurnal precipitation in the US Great Plains were examined with the two-dimensional (2D) Goddard Cumulus Ensemble (GCE) cloud-resolving model (CRM). The model was constrained by the observed large-scale background state and surface flux derived from the Department of Energy (DOE) Atmospheric Radiation Measurement (ARM) Program's Intensive Observing Period (IOP) data at the Southern Great Plains (SGP). The model, when continuously-forced by realistic surface flux and large-scale advection, simulates reasonably well the temporal evolution of the observed rainfall episodes, particularly for the strongly forced precipitation events. However, the model exhibits a deficiency for the weakly forced events driven by diurnal convection. Additional tests were run with the GCE model in order to discriminate between the mechanisms that determine daytime and nighttime convection. In these tests, the model was constrained with the same repeating diurnal variation in the large-scale advection and/or surface flux. The results indicate that it is primarily the surface heat and moisture flux that is responsible for the development of deep convection in the afternoon, whereas the large-scale upward motion and associated moisture advection play an important role in preconditioning nocturnal convection. In the nighttime, high clouds are continuously built up through their interaction and feedback with long-wave radiation, eventually initiating deep convection from the boundary layer. Without these upper-level destabilization processes, the model tends to produce only daytime convection in response to boundary layer heating. This study suggests that the correct simulation of the diurnal variation in precipitation requires that the free-atmospheric destabilization mechanisms resolved in the CRM simulation must be adequately parameterized in current general circulation models (GCMs) many of which are overly sensitive to the parameterized boundary layer heating.

Keywords Diurnal cycle · Nocturnal precipitation · Cloud-resolving model · Cloud-radiation feedback

1 Introduction

It has been a well-recognized problem that most of the current general circulation models (GCMs) exhibit substantial biases in their simulation of the diurnal cycle of warm season precipitation. Deep convection tends to develop too early over land, where they produce too much rainfall in the daytime and too little precipitation during the nighttime (e.g., Ghan et al. 1996; Dai et al. 1999; Zhang 2003; Collier and Bowman 2004; Dai and Trenberth 2004; Dai 2006; Lee et al. 2007a, b, c). This problem extends beyond GCMs to impact the quality of many data assimilation products (those that require the GCMs for a first guess field), suggesting there exists a common, intrinsic problem that is difficult to correct with observations and is apparently associated with deficiencies in the parameterized model physics (Lee and Schubert 2008).

M.-I. Lee
University of Maryland Baltimore County,
Baltimore, MD, USA

M.-I. Lee (✉) · W.-K. Tao · S. D. Schubert
NASA Goddard Space Flight Center,
Mail Code 610.1, Greenbelt, MD, USA
e-mail: myong-in.lee@nasa.gov

I. Choi · I.-S. Kang
School of Earth and Environmental Sciences,
Seoul National University, Seoul, Korea

Published online: 11 February 2009

A number of previous studies suggest that the central problem has to do with deficiencies in the deep convection scheme (e.g., Xie and Zhang 2000; Zhang 2003; Lee et al. 2007a among many others). The predominance of daytime precipitation over land suggests that the models are overly sensitive to the diurnal heating in the planetary boundary layer (PBL). A majority of the convection schemes currently implemented in GCMs are based on a closure assumption tied to the convective available potential energy (CAPE) (e.g., Arakawa and Schubert 1974). CAPE is defined as the amount of energy an air parcel would have if lifted a certain distance vertically through the atmosphere. It measures the convective instability of a given column (basically influenced by both the boundary layer and free-atmospheric large-scale processes), and is most efficiently built up during the daytime as the PBL grows with the heating at the ground. On the other hand, CAPE is reduced and convection is suppressed in the model during the night in association with the large negative buoyancy linked to nighttime surface cooling. In order to overcome this large negative buoyancy, a certain external source of energy must be provided for triggering convection (Kain and Fritsch 1992). In this regard, Xie and Zhang (2000) argued that CAPE would be a necessary, but not a sufficient condition for initiating deep convection.

It is clear that there must exist other destabilization mechanisms in nature that complicate the diurnal response of deep convection. In particular, it appears that the large-scale circulation plays an important role in suppressing, triggering, organizing and dissipating the convective systems (e.g., Silva Dias et al. 1987; Higgins et al. 1997; Carbone and Tuttle 2008). Those mechanisms are often implemented as ad hoc convection triggers and/or inhibition functions that are meant to be simple surrogates for nature's more complex large-scale controls on the deep convection (e.g., Xie and Zhang 2000; Zhang 2003; Lee et al. 2008). For example, several models have incorporated a dependency on the large-scale vertical motion in such a way as to trigger deep convection or expedite the consumption of the convective instability in the presence of large-scale ascending motion (e.g., Fritsch and Chappell 1980; Kain and Fritsch 1992; Pan and Wu 1995; Hong and Pan 1998). Such implementations are usually incomplete, however, and have only shown marginal improvements to the simulated diurnal cycle. Indeed, the two-way interaction between the large-scale environment and convection remains as an unresolved problem, limiting our ability to parameterize the process of deep convection in coarse-grid GCMs. The above discussion suggests that there is a need for a more comprehensive framework that could facilitate an improved understanding of the linkages between convection and the large-scale environment.

Cloud-resolving models (CRMs) have definite advantages over parameterized GCMs in studying the impacts of large-scale environments on the development of cumulus convection, since they do not include any causality assumption between them. Those models are now being widely tested and embedded in several GCMs in place of parameterized convection and cloud processes (often referred to as *superparameterization*, Grabowski and Smolarkiewicz 1999; Randall et al. 2003). CRMs are also used for diagnosing problems with the GCM parameterizations (e.g., Guichard et al. 2004; Chaboureau et al. 2004; Xie et al. 2005). In this study, we investigate the important forcing mechanisms that drive the diurnal variation in convection, with a specific focus on examining the roles of the boundary heating and the large-scale dynamics in initiating deep convection.

Using the CRM, we specifically target the simulation of summertime precipitation over the US Great Plains. One of our primary objectives is to enhance our understanding of the observed nocturnal precipitation maximum in that region (Wallace 1975)—a region where most GCMs fail to capture this pronounced signal. Previous observation studies suggest that several mechanisms could explain the nocturnal precipitation maximum over the US Great Plains. One distinctive feature is the systematic delay in timing of the diurnal precipitation maximum eastward from the Rockies to the adjacent Plains (Riley et al. 1987; Carbone et al. 2002; Nesbitt and Zipser 2003; Carbone and Tuttle 2008; etc.). Carbone et al. (2002) suggested that nocturnal precipitation over the Plains is mainly associated with eastward propagating convective episodes, where the propagation speed is close to that of gravity waves. In an updated observational study, Carbone and Tuttle (2008) confirmed their previous findings and suggested that nocturnal precipitation is primarily determined by (1) the passage of eastward-propagating rainfall systems that form over the mountains; (2) the nocturnal reversal of a mountain–plains circulation; and (3) nocturnal moisture convergence driven by the low-level jet. In fact, the role of the nocturnal low-level jet has been emphasized in many other studies (e.g., Helfand and Schubert 1995; Ghan et al. 1996; Higgins et al. 1997; Schubert et al. 1998), highlighting the important regulation of diurnal convection on sub-continental scales.

Our goal in this study is to improve our understanding of the mechanisms that drive the diurnal cycle of Great Plains precipitation, with the broader goal of improving the parameterization of the mechanisms that drive the diurnal cycle in current GCMs. We use a two-dimensional (2D) CRM with a zonal-vertical domain, forcing it with the observed large-scale fields derived from the atmospheric radiation measurement (ARM) observations at the Southern Great Plains (SGP) sites. In particular, the forcing

consists of three-hourly observations that include the large-scale winds, the large-scale advection of temperature and mixing ratio of water vapor, and the surface sensible/latent heat fluxes (spatially uniform over the horizontal grids). We note that a version of the CRM similar to this was used by Sui et al. (1998) and Tao et al. (2003) to study the mechanisms of diurnal precipitation over the tropical oceans.

2 Model and experiments

The model used in this study is the latest version of the Goddard Cumulus Ensemble (GCE) model (Tao et al. 2003), originally developed by Tao and Simpson (1993). It is an elastic, non-hydrostatic, cloud-resolving model with detailed cloud microphysics that facilitates the study of the development of mesoscale convective systems and their interactions with large-scale dynamics. Prognostic variables include winds, potential temperature, perturbation pressure, turbulent kinetic energy, and mixing ratios of all water phases (vapor, liquid and ice). The model has various options for the ice cloud microphysics. The three-class ice (3ICE) scheme was used for this study, which treats ice cloud, snow, and hail explicitly. The shortwave and longwave radiation schemes are fully interactive with clouds based on a comprehensive parameterization of optical properties for various types of hydrometeors (Tao et al. 1996). The sub-grid scale turbulence parameterization is based on Klemp and Wilhelmson (1978) and Soong and Ogura (1980). Other details of the model are described in Tao et al. (2003) and the references therein.

The GCE model has been tested extensively both in 2D (e.g., Johnson et al. 2002) and three-dimensional (3D) configurations (e.g., Tao and Simpson 1989; Lang et al. 2007; Zeng et al. 2007). In this study, we used the 2D (zonal and vertical) version. The model extends horizontally over a 128 km-long zonal domain with 1-km grid spacing, and vertically from the ground up to 20 km with 41 vertical levels. The time step is 6 s. The CRM is run with cyclic lateral boundary conditions—an option that is commonly used to avoid reflection of gravity waves at the lateral boundaries and allow multi-day integrations. The model is forced only by the prescribed large-scale advection over the domain (there are no extra heat and moisture sources), and therefore avoids any unnecessary complications that would otherwise arise in computing the momentum and heat budgets (Soong and Tao 1980). We note that the domain size of 128 km is relatively small, and the horizontal resolution of 1 km is moderate, compared with other recent CRM studies. However, the results are qualitatively consistent with those from runs with larger domains (tested up to 512 km) and finer resolution (see "Appendix"). Johnson et al. (2002) and Khairoutdinov and Randall (2003) found a similar sensitivity to the changes in the domain size and resolution in their CRM experiments.

This study investigates the response of the GCE model to the prescribed large-scale forcing derived from observational data, which varies continuously in time. We used the ARM IOP single-column model forcing data at SGP to drive the GCE and validate the model simulation. These data contain three-hourly vertical sounding observations that were post-processed into area-averaged single profiles using an objective analysis scheme developed by Zhang and Lin (1997). The values represent the mean ARM cloud and radiation test best (CART) domain rather than a single point (Zhang et al. 2001). The forcing data also provide the surface latent and sensible heat fluxes derived from site-wide averages of observed fluxes from the ARM energy balance bowen ratio (EBBR) stations. The reader is pointed to the description in Zhang et al. (2001) for the details in the objective analysis procedure and the input data source from various observations.

The first set of GCE experiments consists of model simulations with continuous observational forcing over each IOP period. Three IOPs were selected for studying the warm-season convective episodes and their time–mean diurnal variation. These consist of the summer periods of 1995, 1997 and 1999. Each case has a different observing duration but together they make up about 55 days of observations. The large-scale forcing includes the zonal and meridional winds, vertical motion, and advection tendencies of temperature and moisture (water vapor mixing ratio), which were prescribed uniformly over the model domain. For simplicity, surface sensible and latent heat fluxes were also prescribed uniformly by assuming homogenous surface characteristics in the lower boundary over the computation domain. The observed hourly surface precipitation provided by the ARM forcing dataset was used to validate the domain-averaged precipitation simulated by the GCE model. These data are based on the Arkansan Basin Red River Forecast Center (ABRFC) 4-km gridded rainfall analysis, which in turn are based on radar measurements that have been adjusted by the surface rain gauge observations. The study also makes use of the observed cloud fraction at the ARM SGP obtained from the Cloud Modeling Best Estimate (CMBE) dataset. This hourly cloud fraction was derived from the combined estimate of the ARM millimeter-wave cloud radars (MMCR), micropulse lidars (MPL), and laser ceilometers measurements, and vertically gridded to a resolution of 45 m beginning at 195 m above the ground.

The second set of GCE experiments consists of more idealized simulations in which the model is constrained with the same repeating diurnal variation of the large-scale advection and/or surface latent and sensible heat fluxes.

These are designed to discriminate between the mechanisms that determine daytime and nighttime convection. The prescribed forcing in this case was obtained by averaging the time-varying ARM forcing over all the IOPs, while retaining the diurnal variation. Sect. 3.2 provides further details about the experimental setting.

Our approach is analogous to the single-column model approach used in GCMs. Cloud systems are explicitly simulated in CRMs, and their collective responses as represented by a domain average can be straightforwardly compared with the single-column GCM simulation that is driven by identical large-scale advection and surface flux. A key limitation of this approach is in representing the observed eastward propagation of mesoscale convective systems, which, as noted earlier, is one of the important processes contributing to the nocturnal precipitation over the US Great Plains (Maddox 1980; Riley et al. 1987; Carbone et al. 2002; Nesbitt and Zipser 2003). Specifically, a CRM with cyclic boundaries cannot adequately represent the propagation of waves or precipitating systems into the domain from the outside. Those influences are only crudely included in the prescribed large-scale advection forcing. Khairoutdinov and Randall (2003) indicate that the CRM can severely underestimate the cloud fraction possibly because of its inability to account for the lateral advection of clouds over the ARM site. Nevertheless, the results of this study should be valuable for identifying the key processes that drive the diurnal cycle of convection, and should be useful for improving the convective parameterizations in current GCMs.

3 Results

3.1 Test in the realistic case

We first examine the ability of the GCE model to reproduce various precipitation events that occurred during the three summertime ARM IOPs, in response to the observed time-varying large-scale atmospheric and surface boundary forcing. Figure 1 compares the time variations of the observed and simulated precipitation. The model simulation captures the temporal evolution of precipitation events and their magnitudes. For example, the model captures the strong daily precipitation episodes during the early 1995 IOP (19–26 July), followed by the dry period (27–31 July), and then followed by the longer-lasting wet period (1–3 August). The model also shows reasonable simulations for the other two IOPs, except for a few specific events (for example, in 6–8 July 1997 and 16 July 1999).

Although the model simulates the observations reasonably well, particularly for the strongly forced precipitation variability that occurs on the time scale of a few days, it does less well in simulating the diurnal variations. For example, during 20–26 July 1995, when the observation shows very regular nocturnal precipitation events, the model captures only half of those events with accurate timing. The remaining events are misrepresented as daytime events. To get a better sense of the simulated diurnal cycle of precipitation, we constructed a time–mean 24-h diurnal time series by averaging the precipitation amount hour by hour over the entire 55 days. Those results are

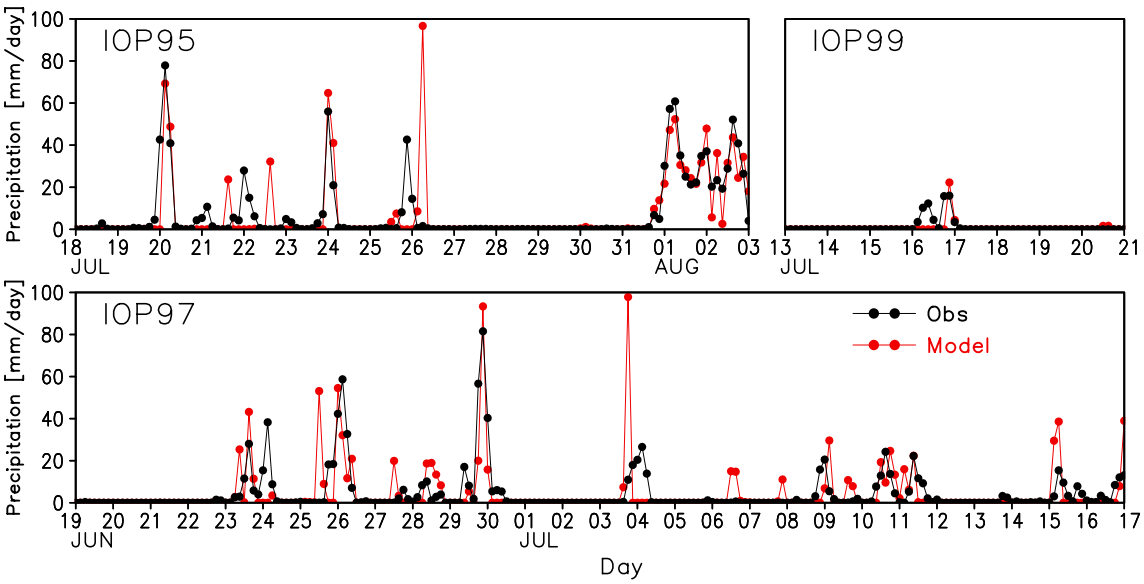

Fig. 1 Time series of three-hourly precipitation (mm day^{-1}) from the observation (*black*) and the GCE model simulation (*red*) during three ARM IOPs in 1995, 1997, and 1999. The observation represents the area average of precipitation over the ARM SGP ground stations, whereas the model simulation is the average over the whole computational domain

shown in Fig. 2a and c. The observed precipitation amount shows a clear maximum in the nighttime centered on local midnight (Fig. 2a), which is consistent with the results from other observational studies that analyzed longer precipitation records (e.g., Higgins et al. 1997). This feature is more or less reproduced in the model simulation (Fig. 2c), but with a much smaller difference between the daytime and nighttime values. On the other hand, the precipitating events, defined as the periods with precipitation greater than 1 mm day^{-1} for a given time of the day, are more frequent during the late evening and nighttime in the ARM observations (Fig. 2b), whereas the model shows the largest frequency in the afternoon (Fig. 2d). Overall, the diurnal variation of the model precipitation from the 55-day long time series is relatively flat and less prominent compared with the observations.

The above deficiencies in the simulated diurnal cycle of precipitation is consistent with what is found in many single-column GCM simulations, although the GCMs exhibit even stronger daytime precipitation (e.g., Guichard et al. 2004). This deficiency is likely in part due to the fact that the model configuration does not explicitly account for the convective systems propagating into the domain—a feature that is also not present in single-column GCMs. In the absence of convection propagating into the domain, the CRM requires explicit forcing to drive nocturnal convection, which in this case comes from the prescribed large-scale advection. This motivates us to turn to longer-time integrations of the GCE model with idealized forcing from observations of the diurnal cycle to help gain further insights into the diurnal precipitation mechanisms. The interpretation is that the CRM is responding as if it were a GCM grid cell to correct diurnal temperature and moisture tendencies. This provides a useful framework for testing mechanisms that could be inserted into a GCM to produce an improved simulation of the diurnal cycle of precipitation.

3.2 Idealized cases

Four idealized experiments were conducted with the GCE model and those are summarized in Table 1. Each experiment was integrated for 100 days, which was long enough to obtain equilibrated statistics. In the first experiment (hereafter EXP1), the model was driven by the observed ARM background forcing, consisting of the 46-day averages of IOP95 and IOP97 but retaining the diurnal variation—we excluded the IOP99 in the average, simply

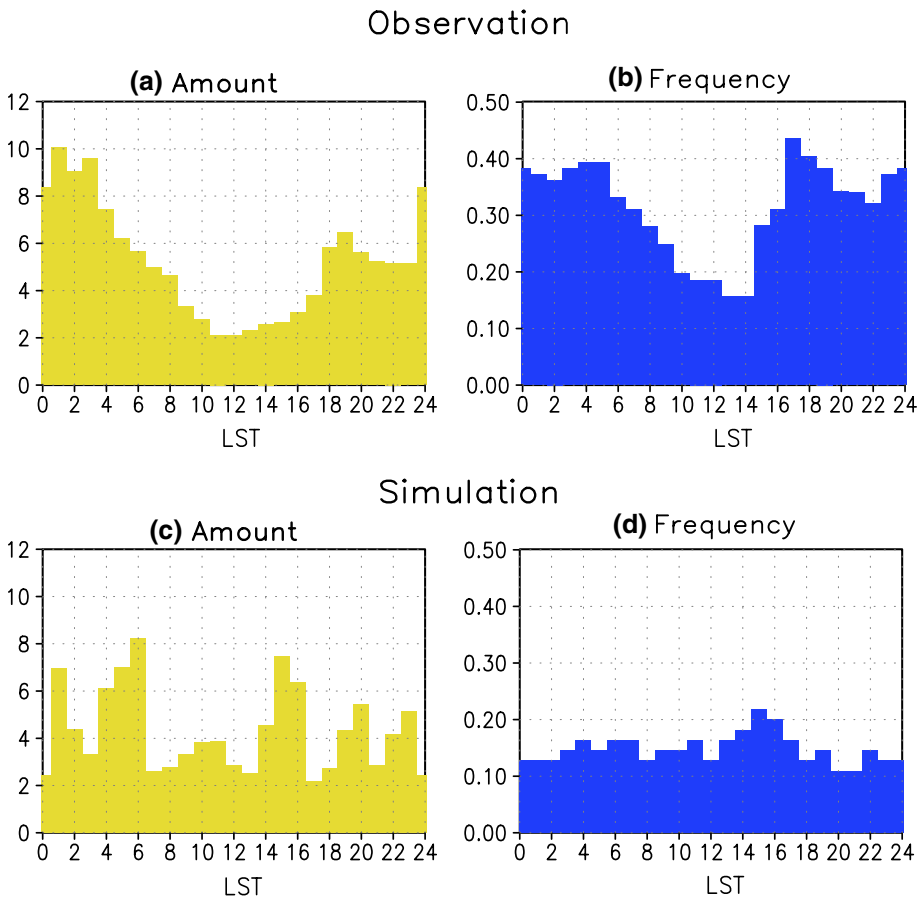

Fig. 2 Diurnal variations of the precipitation amount (mm day^{-1}) and the frequency of precipitation events larger than 1 mm day^{-1}. **a** and **b** are the amount and frequency from the observation and **c** and **d** from the model simulation, respectively

Table 1 A description of the large-scale forcing prescribed to the model in the four idealized experiments

Experiment	Forcing
EXP1	Diurnally varying large-scale advection and surface flux
EXP2	Diurnally varying surface flux with no large-scale advection
EXP3	Diurnally varying large-scale advection with no surface flux
EXP4	Constant large-scale advection and surface flux

because of its short observing period having only one precipitating event. Therefore, the variability of time scales longer than a day is suppressed in the background forcing by design. Figure 3 shows the time-averaged large-scale advection of moisture and temperature (horizontal and vertical advections combined), vertical motion, and sensible and latent heat fluxes. Those were prescribed in the EXP1 run during the entire integration period. The second (EXP2) and the third (EXP3) experiments examine the individual role of the large-scale atmospheric destabilization process and the surface flux in driving the diurnal variation of precipitation. The EXP2 run used the same diurnally varying surface flux as EXP1 but with no large-scale advection, whereas the model was driven with the diurnally varying large-scale atmospheric forcing in EXP3 but with no surface flux. In the last experiment (EXP4), the diurnal variations of the large-scale forcing and the surface flux were averaged out from the configuration of EXP1, and the model was driven by time-invariant forcing.

Diurnal variations of the precipitation amount and frequency from the four experiments are compared in

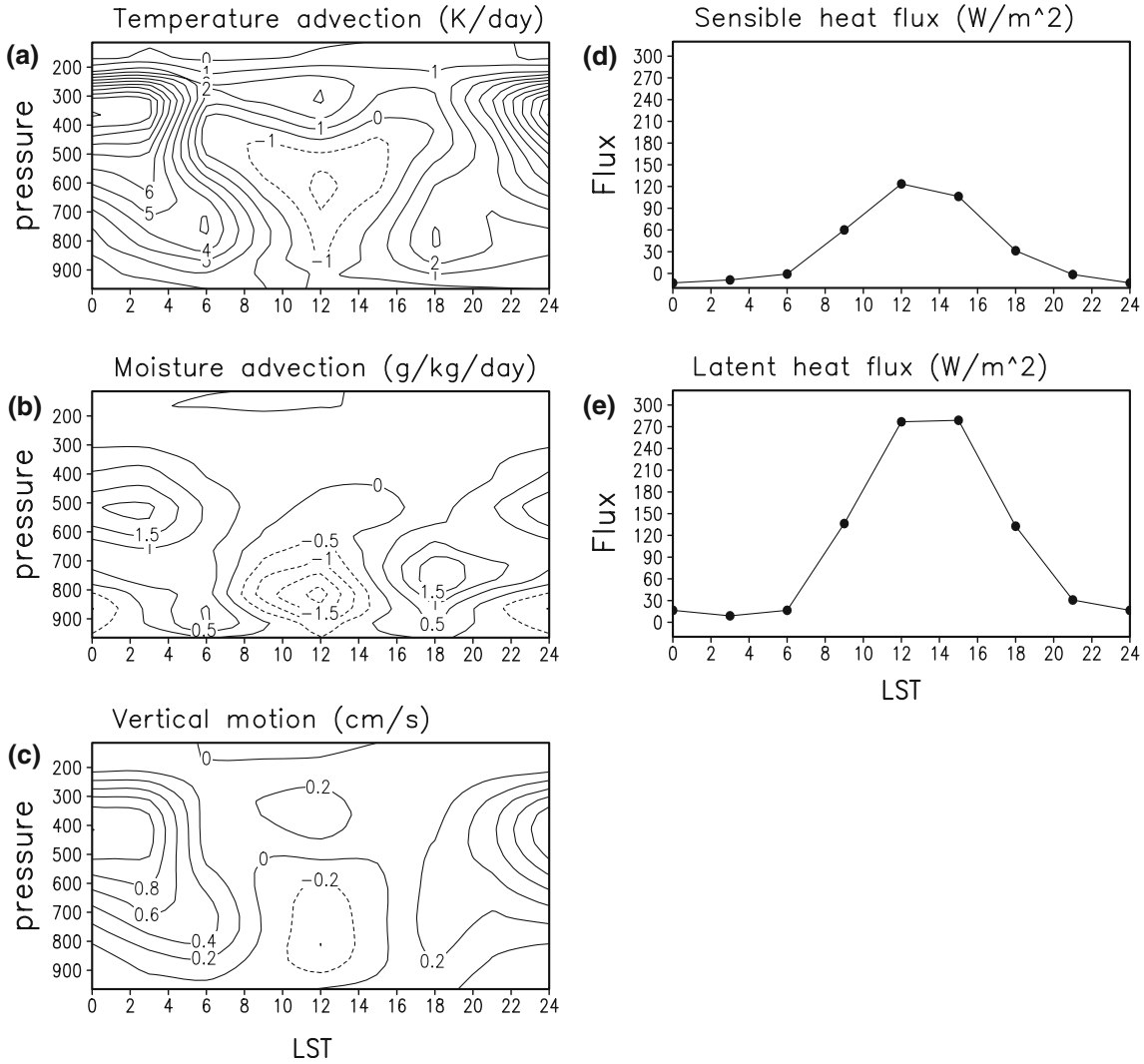

Fig. 3 Time–mean diurnal variations of the large-scale advection tendencies of **a** temperature (K day^{-1}) and **b** moisture (g kg^{-1} day^{-1}) **c** vertical motion (cm s^{-1}), and the surface **d** sensible and **e** latent heat fluxes (W m^{-2}). The values are the averages of 46 days during the ARM 1995 and 1997 IOPs

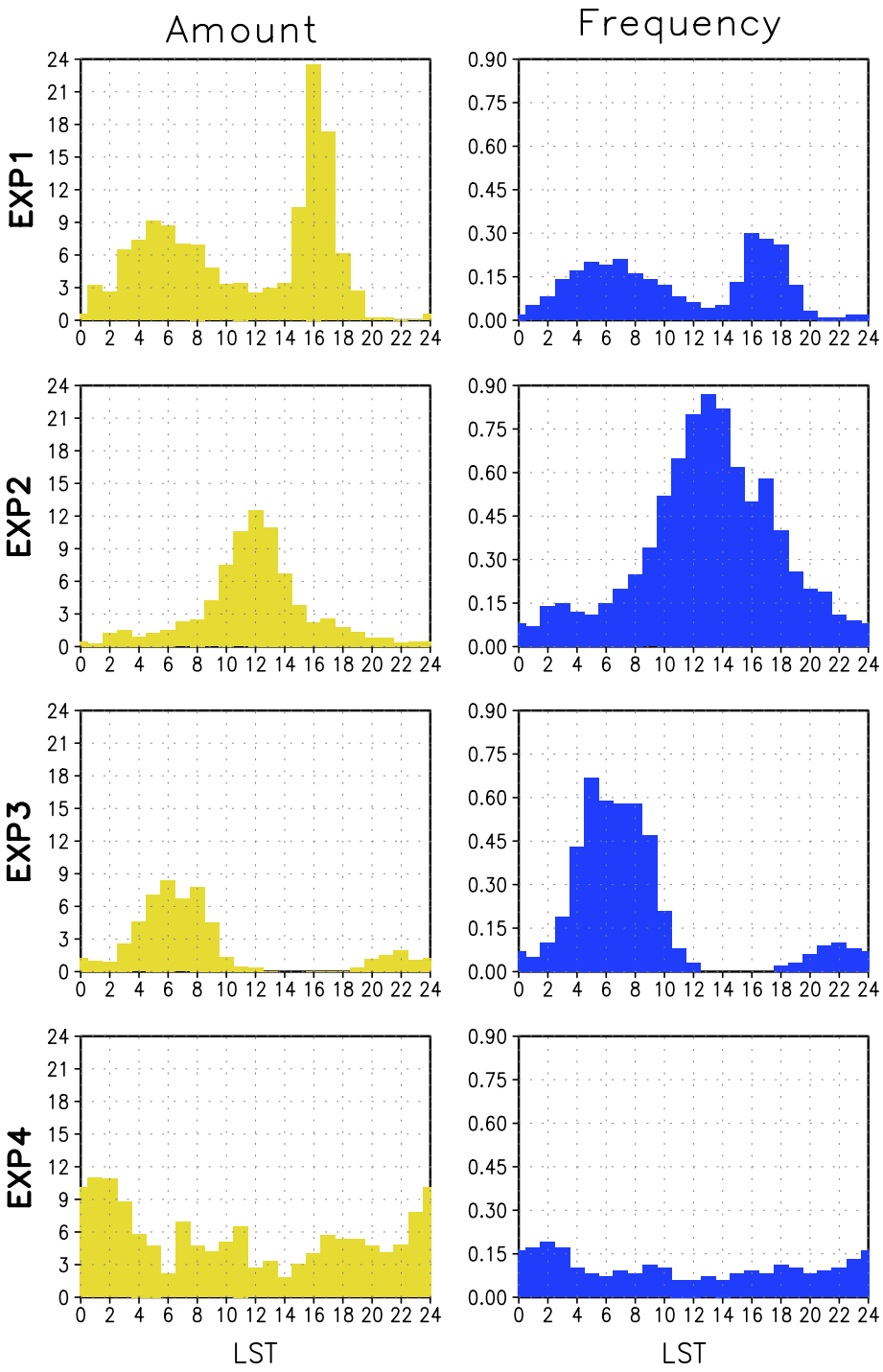

Fig. 4 Diurnal variations of the precipitation amount (*left panels*, unit: mm day^{-1}) and the frequency of precipitation events larger than 1 mm day^{-1} (*right*) from the four idealized runs

Fig. 4. Note that the time–mean total precipitation amount is approximately the same in EXP1 and EXP4 (5.6 mm day^{-1}), which is close to the sum of the other two experiments (EXP2: 3.3 and EXP3: 2.2 mm day^{-1}). In all cases the timing of the peak in the diurnal cycle of precipitation amount is consistent with the peak in the frequency. All of the experiments show clear diurnal variations with, however, different peak timing. It is interesting to see that EXP1 shows two peaks, one in the afternoon (around 1600 LT) and the other during the night (around 0500 LT). It turns out that this bimodal peak is simply a superposition of two distinct precipitation events (see next subsect.). On the other hand, EXP2 shows a single peak at noon. The diurnal variation is quite opposite to that in EXP3, where the nocturnal precipitation is dominated by a peak at 0600 LT with almost no precipitation in the afternoon during 1300–1700 LT. When the prescribed large-scale advection and the surface flux

contain no diurnal variations (EXP4), the diurnal variation of precipitation is substantially suppressed. This suggests that those are the key processes to driving the diurnal variation of precipitation in this cloud-resolving model. Note that, although not very prominent, the model does tend to produce slightly more rainfall in the nighttime in EXP4. We found that with time-invariant forcing the model atmosphere becomes gradually unstable particularly through the constant surface flux in the boundary layer until it finally triggers convection to stabilize the atmosphere. Although the time-invariant surface flux eliminates the influence of diurnally varying surface solar radiation, the model atmosphere is still free to change by radiation. In this case the atmospheric longwave cooling can decrease the stability at night and provide a favorable condition for the nocturnal precipitation. On the other hand, atmospheric shortwave heating can increase the stability during the daytime.

The results from these idealized experiments provide evidence for two distinct mechanisms—one that drives the daytime convection and another that drives nighttime convection. The diurnal variation of surface flux is mainly responsible for the development of convection in the afternoon. The sensible and latent heat fluxes reach their maxima around local noon time (Fig. 3), which induce the PBL heating to increase the convective available potential energy (CAPE). Note that the precipitation frequency reaches up to 80–90% during the peak time in EXP2, which suggests that the convection develops almost every day. This feature basically corresponds to the behavior of many GCMs based on the CAPE-type closure for deep convection (e.g., Lee et al. 2007a, b, c). On the other hand, the mechanisms responsible for nocturnal precipitation must be largely related to the diurnal variation of large-scale atmospheric forcing, since the nocturnal precipitation events simulated in EXP1 disappeared in EXP2 and reappeared in EXP3. The nocturnal peak is more pronounced in EXP3 when compared with EXP4, which suggests that the large-scale advection acts to further destabilize the atmosphere in the nighttime in addition to the nocturnal longwave cooling.

The maximum development of precipitation between late night and early morning in EXP1 and EXP3 coincides with positive moisture advection and large-scale ascending motion in the lower troposphere below 700 hPa (see Fig. 3a–c), which can provide a favorable condition for deep convection. However, whether or not these large-scale atmospheric forcing actually triggers convection is not clear. Indeed the forcing includes a semi-diurnal component with the other peak occurring in the evening (1600–2000 LT), which is not necessarily accompanied by precipitation. Instead, the simulated nocturnal precipitation occurs after a large increase of moisture and ascending motion that peaks at 500 hPa during the nighttime due to large-scale advection. Understanding the nocturnal precipitation mechanisms requires further analysis, which we discuss next.

4 Discussion

In order to better understand the mechanisms for the daytime and nighttime precipitation, we examine EXP1 in more detail. Figure 5 shows the diurnal composites of precipitation and vertical distribution of clouds for the daytime and the nighttime precipitation days. For the daytime composite, we first calculated the hourly time series of domain-averaged precipitation and cloud condensates, and then averaged over the days when the precipitation exceeded 1 mm day^{-1} during 1400–1800 LT. The nighttime composite was done in a similar way but during 0200–0600 LT. The composite analysis shows that the simulated precipitation events are well separated between the daytime and the nighttime cases, implying that the bimodal peaks in Fig. 4a are simply a superposition of two distinct cases. The typical duration of the precipitation is 3–5 h for most of the simulated storms. The composites also show that the daytime precipitation events mostly develop after 1400 LT, reaching their diurnal maximum within 2 h or about 1600 LT. The decaying stage is slower than the developing stage, taking about 4 h before the systems finally dissipate at 2000 LT. The fast developing stage of precipitation is associated with deep convective clouds rooted in the PBL, whereas the cumulus anvil-type high clouds are associated with the slowly decaying stage. This seems to represent a typical evolution of deep convection over land in the GCE. On the other hand, the nighttime rainfall cases involve precipitation more widely spread in time from midnight to noon local time with a maximum at around 0400–0600 LT, and with an amplitude that is weaker than for the daytime convection case. We found that the wide spread in time of precipitation does not necessarily indicate a longer duration of individual precipitating events. The composite, in fact, suggests a weaker phase-locking of precipitation with the diurnal cycle than for the daytime precipitation case. Note that mid-to-high clouds form before nocturnal precipitation begins, suggesting a possible role of high clouds in producing *top-down* development of the nocturnal convection, compared with the *bottom-up* evolution of daytime convection.

We next look in more detail at the life cycle of individual storms. Two storms representing the daytime and the nighttime precipitation cases were examined following their movements (Figs. 6, 7). Note that these are grid point values at the center of the storms (defined as the local precipitation maximum), which should be useful for understanding the structure of an individual convective

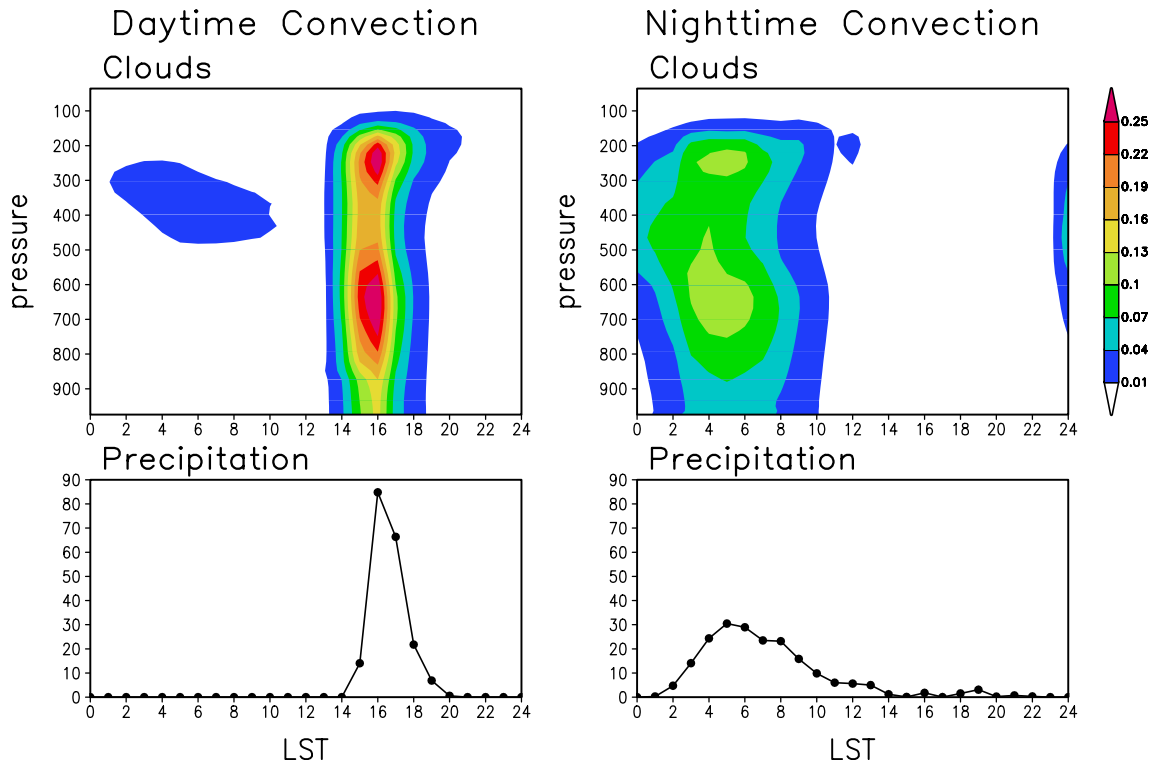

Fig. 5 Diurnal composites of the vertical distribution of cloud, as indicated by the sum of total hydrometeors including cloud water, ice, rain, snow, and hail (*top panels*), and surface precipitation (*bottom*) for the daytime convection (*left*) and the nighttime convection cases (*right*). The units are g kg^{-1} for clouds and mm day^{-1} for precipitation

system such as its vertical motion field, as well as how it interacts with radiation. We found that these cases are good representations of the typical evolution of daytime and nighttime convection simulated by the model. The daytime convection case (Fig. 6) is consistent with the domain-averaged composite (Fig. 5, left panels), in that the convection cell is destabilized from the turbulent boundary layer. The storm initiates vertical motion in the boundary layer, which eventually leads to a vertical flushing of mass throughout the deep column (Fig. 6c). Before the development of deep convection, the atmosphere is free of clouds (Fig. 6a), and the shortwave heating (Fig. 6d) is larger than the longwave cooling (Fig. 6e) by 1–2 K day^{-1}. The shortwave heating is quite uniform in the vertical. As mentioned earlier, the enhanced surface fluxes maximize at local noon and are mainly responsible for the boundary layer heating and the increase in convective instability.

In the nighttime convection case (Fig. 7), there is a significant build-up of high clouds before nocturnal precipitation develops (Fig. 7a). In the absence of shortwave radiation in the nighttime, longwave cooling at the top of clouds and heating from below can effectively increase the convective instability (Fig. 7d, e). The vertical depth of the heating layer associated with high clouds increases as the cloud amount increases (Fig. 7a), and deep convection eventually develops from the boundary layer (Fig. 7c), producing nocturnal precipitation (Fig. 7b). Note that the daytime convection does not immediately follow the nighttime convection in the same day in EXP1. The next precipitating systems tend to develop about one and one half days later in the daytime, suggesting that the model requires some time to rebuild the convective instability.

In explaining the nocturnal convection, the build-up of high clouds during the nighttime is an essential component, but the mechanisms responsible for that are not clear. Considering that they are non-precipitating, stratiform-type clouds, the following processes are hypothesized to help saturate the upper atmosphere: (1) cooling induced by longwave radiation and/or upward vertical motion, and (2) moisture increase by large-scale advection. Both processes increase the relative humidity and may induce a feedback though the interaction of condensational heating and vertical motion. Relating these processes to the prescribed large-scale advection (Fig. 3), mid-to-upper level moisture advection seems to be more responsible in this case for building up high clouds, rather than the temperature advection, which actually shows a tendency for warming. By carrying out additional sensitivity experiments to separate the impacts of horizontal and vertical moisture advection, we found that the vertical moisture advection is critical for driving nocturnal convection in the model. When the vertical moisture advection tendency is

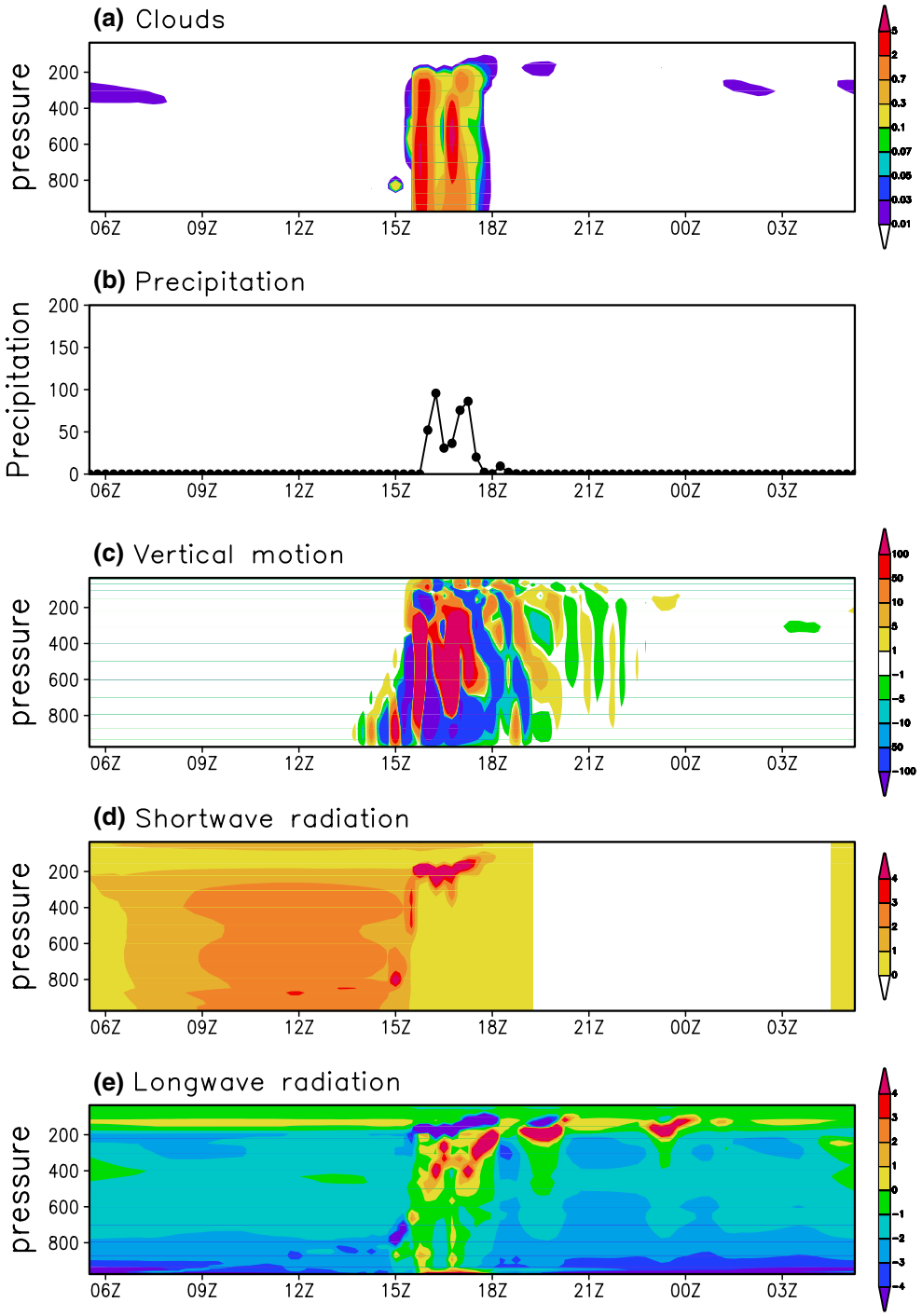

Fig. 6 Life cycle of the storm developed in the daytime. Presented are **a** the total hydrometeors (g kg^{-1}) **b** the surface precipitation (mm day^{-1}) **c** the vertical motion (cm s^{-1}), and the radiation heating rates by **d** shortwave and **e** longwave (K day^{-1}). Values are at the center of the storm (defined as the local precipitation maximum), which progresses eastward in time

eliminated from the prescribed large-scale forcing, the model generates only the daytime convection, reaching its maximum magnitude in the afternoon (1600 LT) (not shown). The ARM observations seem to support this to a large degree. Figure 8 shows the observed vertical advection tendency of moisture and surface precipitation during the periods of strong nocturnal precipitation events (19–24 July) and the quite inactive period of precipitation (26–31 July) in the IOP95. Observed nocturnal precipitation events are mostly associated with increased moisture due to vertical advection. It is, however, unclear from the observations whether the increase of moisture by vertical

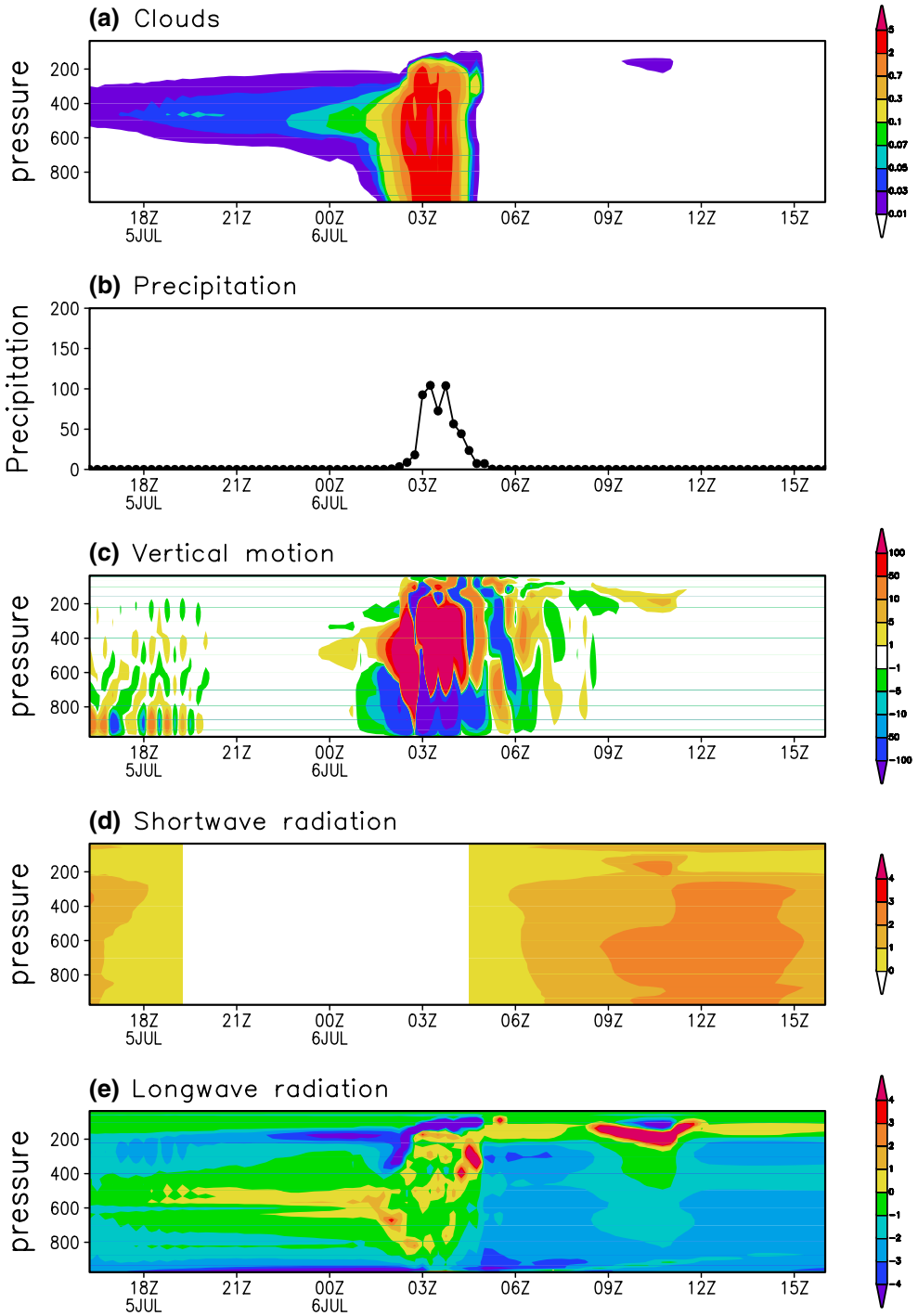

Fig. 7 Same as in Fig. 6 but for the convective storm developed in the nighttime

advection triggers nocturnal precipitation or whether the nocturnal precipitation drives vertical moisture advection. In fact, one cannot easily separate the two processes as they can interact and feedback on each other. However, the GCE model simulation suggests an important role of cloud–radiation feedback between high-cloud and longwave radiation, which further destabilizes the atmosphere and induces deep convective systems in the nighttime.

We tested this hypothesis by conducting additional sensitivity experiments with the GCE model, where we eliminated the radiative impacts of clouds in EXP3 (the case when the nocturnal precipitation is dominant). This was done in the model by assuming zero optical thickness for the cloud in each integration time step. We simulated the cases of no radiative interaction of clouds both in longwave and shortwave radiation, but here we only discuss the former to

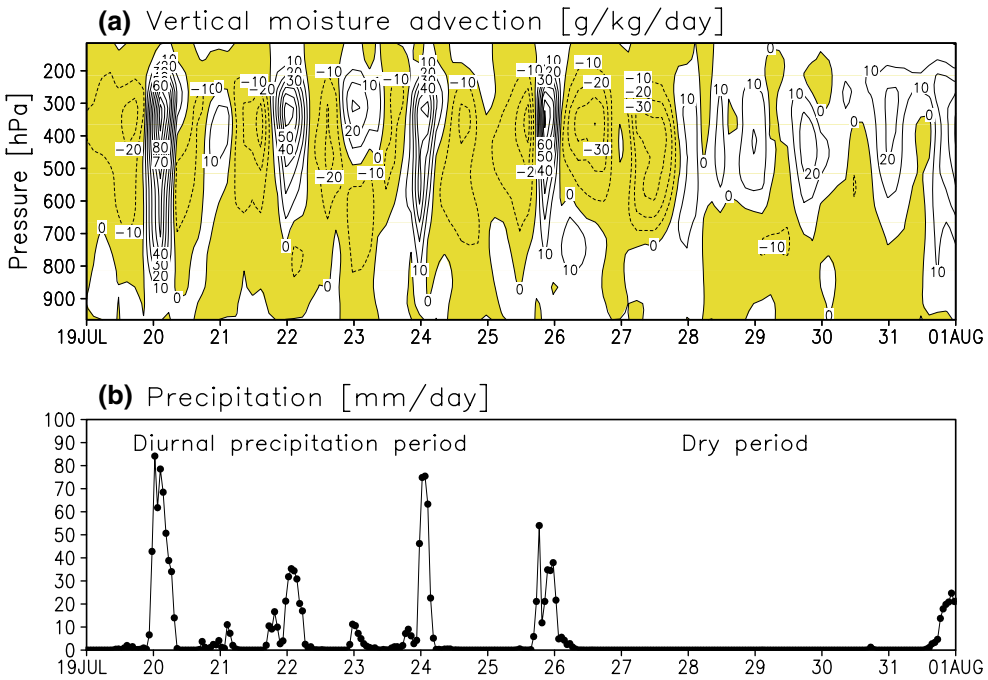

Fig. 8 **a** Time-height variation of the vertical moisture advection of moisture (g kg^{-1} day^{-1}) during 00UTC 19 July–00 UTC 1 August 1995 obtained from the ARM IOP forcing data in the IOP1995. Negative values are *shaded* and contoured in *dashed line*. **b** Shows the time variation of surface precipitation (mm day^{-1}) averaged over the ARM SGP ground stations for the corresponding period

elucidate the role of longwave cloud radiative forcing in the nocturnal precipitation process. Figure 9 shows the diurnal variations of the precipitation amount and the frequency from the experiment with no cloud-longwave radiation interaction. Comparing with EXP3 (shown in the third-row panels in Fig. 4), the amplitude of the diurnal variation of precipitation amount (Fig. 9a) has been reduced by about half from that of EXP3. In this case, the model tends to generate precipitation more frequently during almost every day (Fig. 9b), but with a much reduced intensity in the domain-averaged precipitation (not shown). Without any imposed surface flux, only the nocturnal longwave cooling of the atmosphere acts to drive nighttime precipitation associated with the large-scale advective moisture increase. The sensitivity experiment suggests again that the nocturnal longwave cooling by clouds is working in such a way as to amplify the nocturnal precipitation.

In order to further assess the realism of the model simulations we examine in Fig. 10 the seasonal-mean diurnal variations of cloud fraction and precipitation from the ARM observations. Because of the highly varying nature of clouds in time, we averaged the data over a

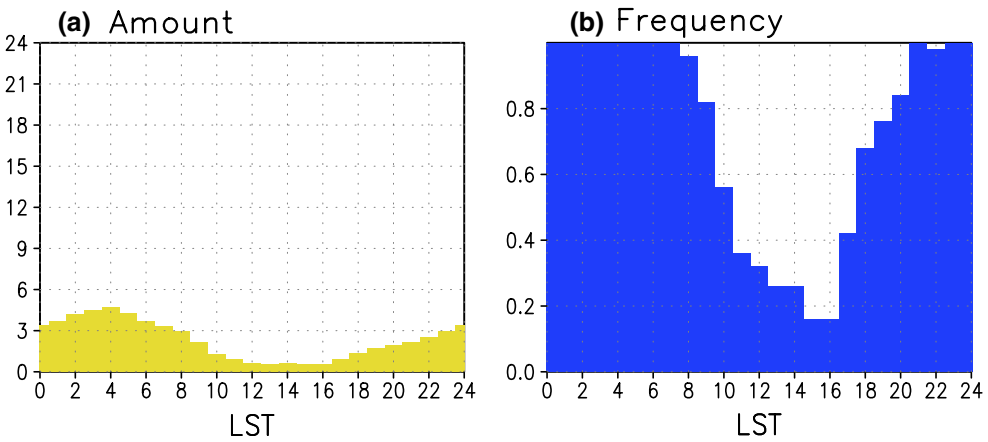

Fig. 9 Diurnal variations of the precipitation **a** amount (unit: mm day^{-1}) and **b** frequency of precipitation events larger than 1 mm day^{-1} from the sensitivity run without longwave cloud radiative forcing in EXP3 (see the text for the detail). The diurnal cycle of precipitation was obtained from the last 50 days from the 100-day model simulation

season (June–July 1997). There is a late evening maximum (18-00 LT) in the diurnal cycle of high-cloud fraction at 9–12 km, which precedes the nocturnal precipitation maximum at 01–02 LT. Just before the time of maximum precipitation the cloud distribution expands downward in the vertical, indicating an active convection regime. This observed feature is qualitatively similar to the model result. In the US Great Plains, the possibility of high-cloud generation by pre-existing cloud systems that are initiated over the Rocky Mountains (Riley et al. 1987; Carbone et al. 2002; Carbone and Tuttle 2008) and moisture transport by the nocturnal low-level jet (Helfand and Schubert 1995; Schubert et al. 1998) should also be considered in contributing to the nocturnal build-up of high clouds. We suggest that those processes are implicitly represented in the imposed large-scale forcing that we use in this study, although the current setup of the CRM cannot adequately account for high-clouds entering into the domain associated with propagating convective systems.

5 Summary and conclusions

The 2D GCE cloud-resolving model was used to help understand the mechanisms that drive the diurnal cycle of precipitation in the summertime US Great Plains. The model was run on a 128-km zonal by 20-km vertical domain and forced with the large-scale background state (i.e., advection tendencies of mass, temperature, and humidity) and surface fluxes (i.e., surface sensible and latent heat fluxes) derived from the ARM observations in the Southern Great Plains. The model captures most of the observed (1995, 1997, and 1999 IOP) rainfall events reasonably well with realistic magnitudes, particularly for the strongly forced events driven by synoptic disturbances. However, the model does less well for the weakly forced diurnal convection events that developed during the night.

Four idealized 100 day GCE simulations were conducted in order to gain further insights into the diurnal precipitation mechanisms. The first experiment (EXP1)

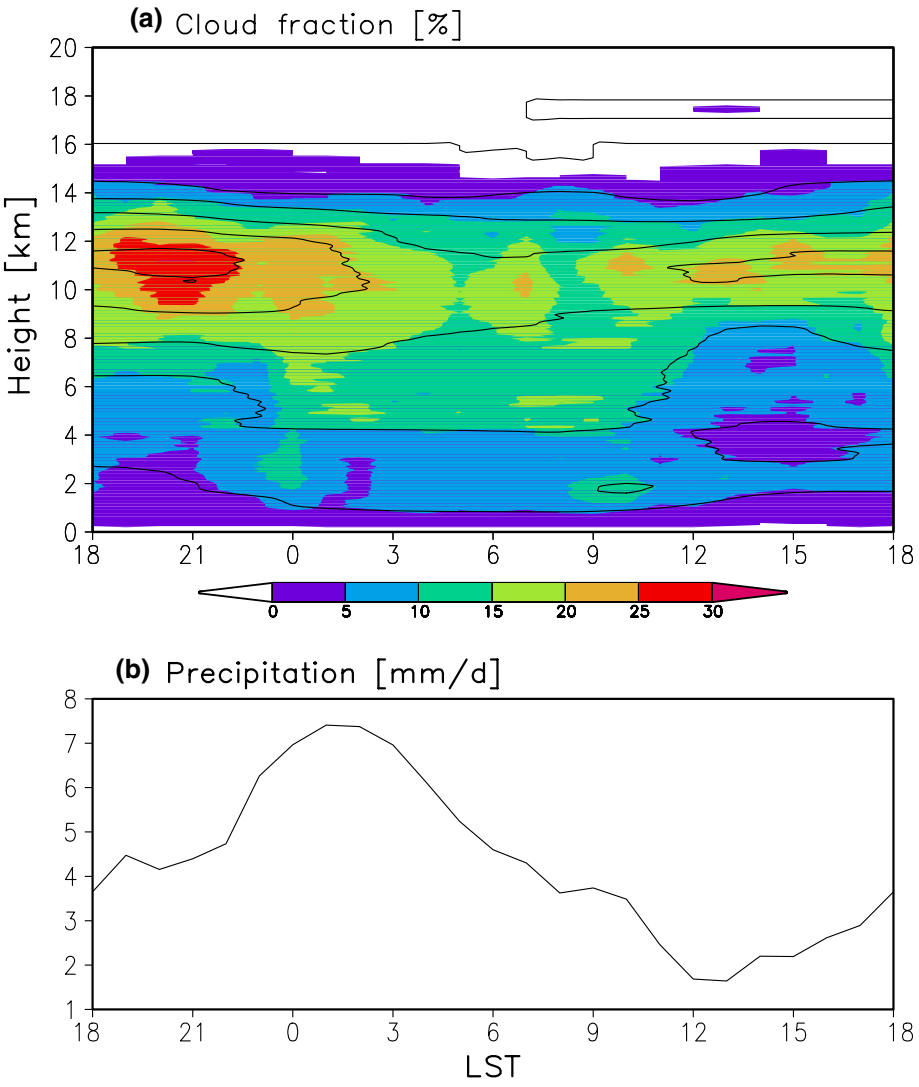

Fig. 10 Observed seasonal-mean diurnal variations of **a** the cloud fraction (%) and **b** the precipitation (mm day^{-1}) at ARM SGP during June–July 1997. The diurnal cycles are obtained from hourly-mean observations. In (**a**), the cloud fraction is shaded in 5% interval with 1-2-1 smoothed contours in the time (local time)-height (km, from ground) domain

was driven by the time–mean diurnal variations in the large-scale atmospheric advection and surface fluxes. The second experiment (EXP2) was provided only with the time–mean diurnal variation of the surface flux, and the third (EXP3) only with the time–mean diurnal variation of large-scale advection. The fourth experiment (EXP4) used the time invariant large-scale advection and surface flux with no diurnal variation. Each model integration revealed a distinctive and robust feature in the simulated diurnal cycle of precipitation. EXP1 is characterized by two peaks in the time–mean diurnal cycle of precipitation, which turned out to be simply a superposition of daytime and the nighttime convection that develops independently. On the other hand, EXP2 shows only the daytime convection, whereas EXP3 shows predominantly nocturnal precipitation. These results suggest that there are two different destabilization processes for diurnal convection. The diurnal variation of the surface flux triggers the daytime development of deep convection, whereas the large-scale dynamical forcing drives the nocturnal convection. This is consistent with EXP4 which shows a very suppressed diurnal variation of precipitation.

The results also highlight the important roles of the large-scale upward motion and associated moisture advection in preconditioning nocturnal precipitation events. These act to saturate the upper troposphere and produce high clouds, which develop ahead of the deep convection. The long-wave radiation interacting with high clouds decreases the vertical stability by cloud-top cooling and cloud-base warming, and eventually triggers nocturnal deep convection. This *top-down* destabilization process is in contrast to the daytime convection where the boundary layer grows by surface heating which eventually triggers deep convection (*bottom-up* destabilization).

The high-cloud destabilization process for triggering nocturnal convection examined here is similar to the mechanisms proposed for oceanic diurnal convection in the deep tropics. Several modeling and observational studies have examined how clouds can interact with radiation such as through cloud-top cooling and cloud-base warming to destabilize the atmospheric column under the stratiform cloud layer (e.g., Webster and Stephens 1980; Randall et al. 1991; Liu and Moncrieff 1998), and/or through differential cooling between clear and cloudy regions to enhance dynamic convergence into the cloud system (e.g., Gray and Jacobson 1977). Using another CRM, Xu and Randall (1995) showed that the diurnal cycle of deep convection over the tropical oceans is basically a direct response to cloud-radiation interactions, in which solar absorption by clouds stabilizes the large-scale environments during the daytime relative to the nighttime. However, their simulated rainfall for both interactive and non-interactive clouds is quite similar, although the interactive case delays the nocturnal peak by a few hours. Liu and Moncrieff (1998) confirmed that the direct interaction between radiation and clouds is the dominant process rather than the cloud/cloud-free differential heating based on their CRM simulation results. They also showed that highly (less)-organized cloud systems with strong ambient wind shear can have strong (weak) diurnal variations of rainfall. Although those previous studies emphasized the important role of direct cloud–radiation interaction, they basically assume preexisting clouds with no explanation as to what processes are responsible for generating clouds in the nighttime. Regarding this, Tao et al. (1996, 2003) suggested an important role of large-scale free-atmospheric cooling in the nighttime by longwave radiation for destabilizing the large-scale environment in the tropics. They suggested that the nocturnal longwave cooling is important for increasing the relative humidity and available precipitable water (Sui et al. 1997, 1998), but not CAPE, in the case of the tropics with high moisture content. Those arguments are generally consistent with the findings in this study. Considering the case of the relatively dry, midlatitude continent, the nocturnal cooling effect alone may not be sufficient to increase the RH. Our GCE model results showed that the *moisture* increase by large-scale advection is required to generate nighttime convection. When the large-scale vertical moisture advection is eliminated, the model generates only afternoon (around 1600 LT) convection.

This study suggests an important role for the free-atmospheric large-scale destabilization process in driving the nocturnal precipitation over the Great Plains. Interestingly, Guichard et al. (2004) and Chaboureau et al. (2004) obtained a somewhat different sensitivity in CRMs with a similar experiment over the Great Plains using the ARM dataset. Their models produce only the afternoon convection. The differences seem to be mainly caused by the differences in the large-scale advection tendencies prescribed to the model, where they selected them from a typical day of afternoon convection case whereas we averaged them over all the observing periods. As a result, their maximum moisture increase by large-scale advection occurs in the early afternoon, when the surface heat fluxes also have the diurnal maximum (compare Fig. 3 of this paper and Fig. 1 of Guichard et al.). Also note that, without the large-scale advection tendencies, the GCE model tends to produce the daytime convection at noon (compare EXP1 and EXP2 in Fig. 3), implying that the daytime subsidence and drying could possibly delay the daytime convection to the late afternoon or evening in the EXP1 case. The daytime subsidence coincides well with the observed widespread downward motion over the Great Plains associated with the descending branch of the thermally driven mountain–plains circulation (Silva Dias et al. 1987; Carbone and Tuttle 2008).

The CAPE-type closure schemes implemented in many GCMs for deep convection have an inevitable difficulty in simulating nighttime convection, as they have to overcome a large nighttime negative buoyancy layer below the LFC (Kain and Fritsch 1992; Lee et al. 2008). This study suggests that in order to overcome this problem, the parameterizations of the cloud–radiation interaction and middle-level convection need to incorporate the free-atmospheric destabilization processes that we have seen in the CRM simulation. In future work we plan to test the 3D GCE model to examine the organization and propagation characteristics of the mesoscale convective systems and their influence on the diurnal cycle of precipitation in the Great Plains.

Acknowledgments We thank Drs. Max Suarez, Julio Bacmeister, Xiping Zeng, In-Sun Song and two anonymous reviewers for their helpful comments and suggestions. This study was supported by NASA's Modeling, Analysis, and Prediction (MAP) program. Ildae Choi and In-Sik Kang were supported by the Korea Meteorological Administration Research and Development Program under Grant CATER_2007-4206 and BK21 program. Wei-Kuo Tao and the GCE model were supported by the NASA Headquarters' Atmospheric Dynamics and Thermodynamics Program and the NASA Precipitation Measuring Mission (PMM). The ARM IOP single-column model forcing dataset were provided by the US Department of Energy as part of the Atmospheric Radiation Measurement (ARM) Program. We thank Shaocheng Xie who kindly provided us with the observed hourly precipitation and the Climate Modeling Best Estimate (CMBE) cloud fraction at the ARM SGP for the model validation.

Table 2 A description of the sensitivity experiments to the domain size and the horizontal resolution

Experiment	Domain ($x - z$)	Horizontal resolution	Integration days
EXP1a	128 − 20 km	250 m	20
EXP1b	256 − 20 km	1 km	20
EXP1c	512 − 20 km	1 km	20
EXP1d	512 − 20 km	250 m	20

Other configurations are exactly same as EXP1 that described in Table 1 and the text

Appendix: Sensitivity tests

Sensitivity experiments were conducted to examine the impact of the domain size and the horizontal resolution changes on the simulated diurnal precipitation variability. For simplicity, we selected the idealized case of EXP1 where the model tends to generate both the daytime and nighttime precipitation from the imposed diurnally varying large-scale advection and surface heat flux. We tested the GCE model in four different settings with different domain sizes and horizontal resolutions, which are summarized in Table 2. Each experiment was run for 20 days for a quick evaluation and we use the last 15 days to examine the diurnal variation. Due to relative short-time integration period, the precipitation frequency exhibits clearer diurnal variation than the precipitation amount, which we compare in Fig. 11. These frequency

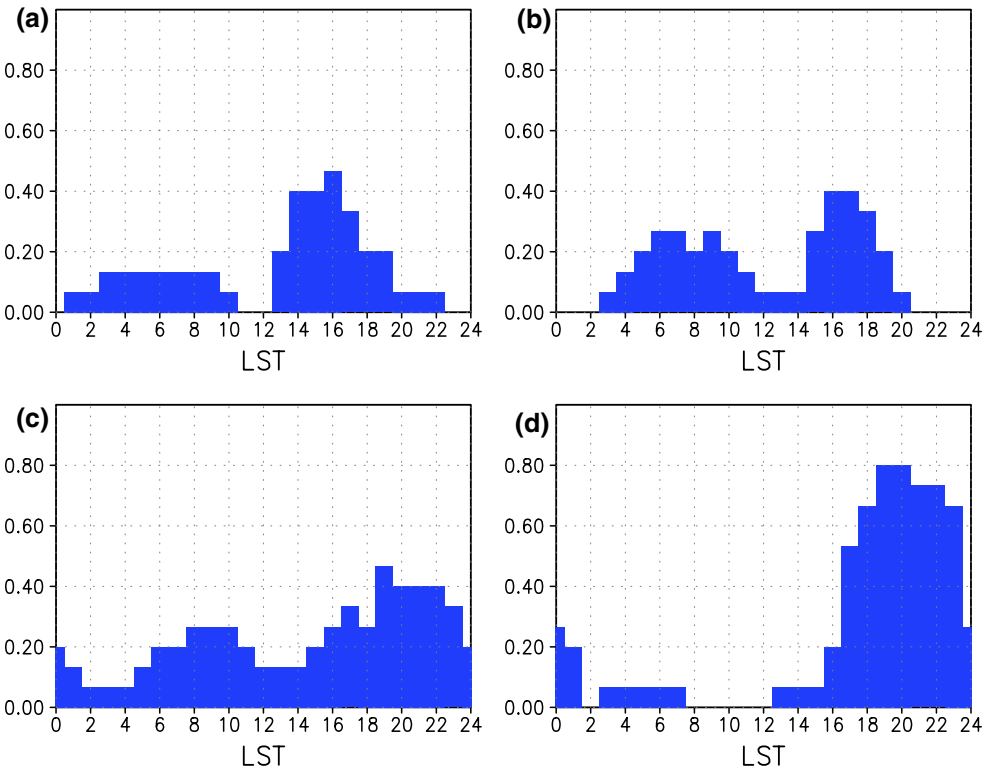

Fig. 11 Diurnal variations of the frequency for the precipitation events larger than 1 mm day^{-1} in the four sensitivity experiments **a** EXP1a **b** EXP1b **c** EXP1c, and **d** EXP1d. The results are calculated for the last 15 days from the total 20-day integrations

statistics are stable when we differ the averaging period. The results show that increasing the horizontal resolution from 1 km to 250 m (EXP1a) does not modify the simulated diurnal cycle of precipitation significantly (compare Fig. 11a with EXP1 in Fig. 4). The domain size seems to have a bigger impact on the phase (timing of the peak) of the diurnal convection. At a domain size of 256 km (EXP1b, Fig. 11b) the results are quite similar to those from the 128-km domain (EXP1). When, however, the GCE domain is extended to 512 km (EXP1c, Fig. 11c), the diurnal peaks tend to be delayed in time both in the daytime and the nighttime precipitation. The delay is largest for the daytime precipitation with the peak shifted into late evening. When we both extend the domain to 512 km and reduce the grid spacing to 250 m, the sensitivity is largest with only a late evening peak (EXP1d, Fig. 11d).

A late evening peak in a bigger domain is intriguing whether it is driven by boundary layer heating or free-atmospheric large-scale advection. To address this issue, we again select a single storm in this case (EXP1d) and examine its temporal evolution following the storm center (Fig. 12). The result is quite consistent with the daytime convection in EXP1 (as shown in Fig. 6). In this case, the simulation has slower transition from shallow to deep convection (Fig. 12c). Surface precipitation (Fig. 12b) reaches its maximum intensity after maximum development of cloud (Fig. 12a) associated with deep convection penetrating through the PBL. We found a similar high-cloud destabilization process in the developing early morning convection in the largest domain run of EXP1c (not shown). Therefore, we conclude that the fundamental mechanisms for diurnal convection that we identified in the control simulations are qualitatively consistent with the experiments with larger domains and finer resolution. This is consistent with the sensitivity tests done with the 2D GCE model by Johnson et al. (2002, see their Fig. 12).

The impact of the domain size and the resolution on the individual storm can be understood better by comparing the Hovmuller plots of precipitation (Fig. 13). The increase of domain and resolution in general tends to increase the lifetime of individual storms that propagate more slowly. This explains the delay in the peak of the diurnal precipitation (Lang et al. 2007). Both in the small and large domain cases, precipitation develops regularly on a diurnal basis, presumably due to the imposed, regular diurnal forcing. We note that, even for the small domain, the cyclic

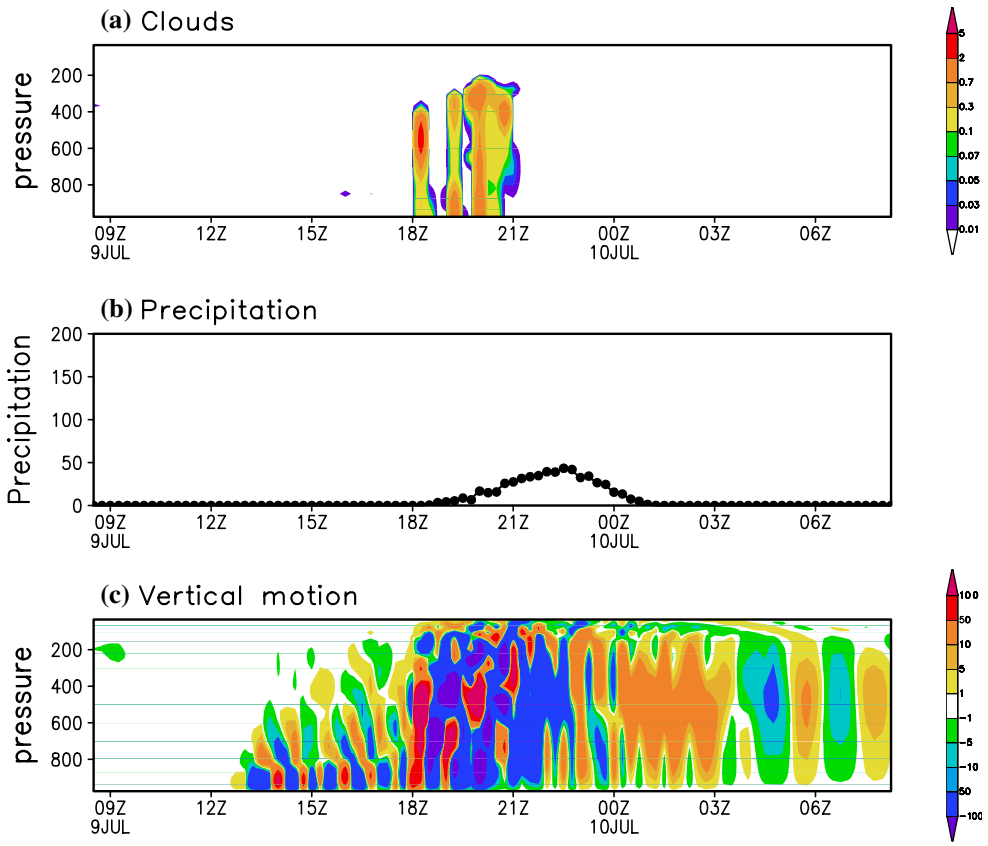

Fig. 12 Life cycle of the storm developed in EXP1d. **a** The total hydrometeors (g kg^{-1}) **b** the surface precipitation (mm day^{-1}), and **c** the vertical motion (cm s^{-1}). Others are same as in Fig. 6a–c

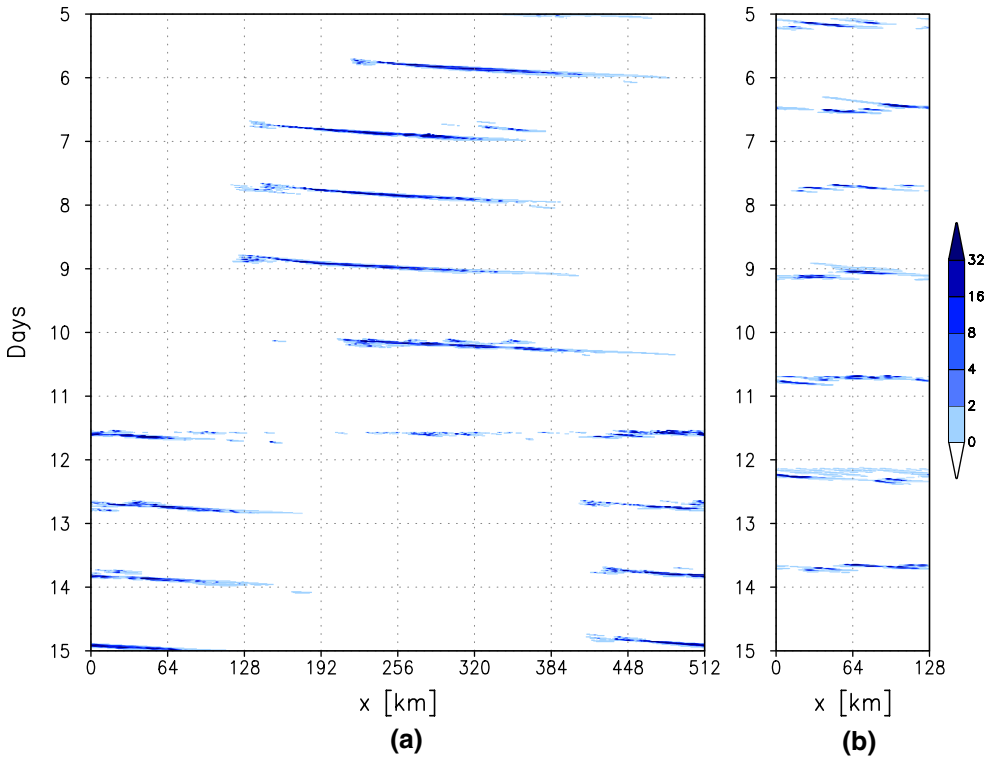

Fig. 13 Hovmuller plots of surface precipitation (mm h^{-1}) from day 5–15 in **a** EXP1d and **b** EXP1

lateral boundary condition in the GCE does not give any unrealistic influence on the diurnal cycle due to the relatively short durations of the simulated storms.

Although we examine the sensitivity for the idealized case, we do not expect drastic changes for the case of more realistic forcing, or for the case of 3D experiments. Khairoutdinov and Randall (2003) tested their CRM with the ARM IOP 1997 single-column model forcing and found that the simulations are rather insensitive to changes in the domain size and the horizontal resolution when these are varied over a wide range. They further indicated that the overall effects of increasing the model dimension from 2D into 3D are minor in terms of the evolution of the simulated domain-mean fields such as precipitation and total precipitable water (see their Fig. 2). They did, however, find more rapid temporal fluctuations in the 2D model compared with the 3D counterpart (Grabowski et al. 1998; Tompkins 2000). They suggested that continuous, strong large-scale forcing in the CRM simulation might constrain the model too much to reveal any model differences.

References

Arakawa A, Schubert WH (1974) Interaction of a cumulus cloud ensemble with the large-scale environment. Part I. J Atmos Sci 31:674–701. doi:10.1175/1520-0469(1974)031<0674:IOACCE>2.0.CO;2

Carbone RE, Tuttle JD (2008) Rainfall occurrence in the United States warm season: the diurnal cycle. J Clim. doi:10.1175/2008JCLI2275.1

Carbone RE, Tuttle JD, Ahijevych DA, Trier SB (2002) Inferences of predictability associated with warm season precipitation episodes. J Atmos Sci 59:2033–2056. doi:10.1175/1520-0469(2002)059<2033:IOPAWW>2.0.CO;2

Chaboureau J-P, Guichard F, Redelsperger J-L, Lafore J-P (2004) The role of stability and moisture in the diurnal cycle of convection over land. Q J R Meteorol Soc 130:3105–3117. doi:10.1256/qj.03.132

Collier JC, Bowman KP (2004) Diurnal cycle of tropical precipitation in a general circulation model. J Geophys Res 109:D17105. doi:10.1029/2004JD004818

Dai A (2006) Precipitation characteristics in eighteen coupled climate models. J Clim 19:4605–4630. doi:10.1175/JCLI3884.1

Dai A, Trenberth KE (2004) The diurnal cycle and its depiction in the community climate system model. J Clim 17:930–951. doi:10.1175/1520-0442(2004)017<0930:TDCAID>2.0.CO;2

Dai AG, Giorgi F, Trenberth KE (1999) Observed and model-simulated diurnal cycles of precipitation over the contiguous United States. J Geophys Res 104:6377–6402. doi:10.1029/98JD02720

Fritsch JM, Chappell CF (1980) Numerical prediction of convectively driven mesoscale pressure systems: part I. Convective parameterization. J Atmos Sci 37:1722–1733. doi:10.1175/1520-0469(1980)037<1722:NPOCDM>2.0.CO;2

Ghan SJ, Bian X, Corsetti L (1996) Simulation of the Great Plains low-level jet and associated clouds by general circulation models. Mon Weather Rev 124:1388–1408. doi:10.1175/1520-0493(1996)124<1388:SOTGPL>2.0.CO;2

Grabowski WW, Smolarkiewicz PK (1999) CRCP: a cloud resolving convection parameterization for modeling the tropical convective atmosphere. Phys D 133:171–178. doi:10.1016/S0167-2789(99)00104-9

Grabowski WW, Wu X, Moncrieff MW, Hall D (1998) Cloud-resolving modeling of cloud systems during phase III of GATE. Part II: effects of resolution and the third spatial dimension. J Atmos Sci 55:3264–3282. doi:10.1175/1520-0469(1998)055<3264:CRMOCS>2.0.CO;2

Gray WM, Jacobson RW (1977) Diurnal variation of deep cumulus convection. Mon Weather Rev 105:1171–1188. doi:10.1175/1520-0493(1977)105<1171:DVODCC>2.0.CO;2

Guichard F et al (2004) Modelling the diurnal cycle of deep precipitating convection over land with cloud-resolving models and single-column models. Q J R Meteorol Soc 130:3139–3172. doi:10.1256/qj.03.145

Helfand HM, Schubert SD (1995) Climatology of the simulated Great Plains low-level jet and its contribution to the continental moisture budget of the United States. J Clim 8:784–806. doi:10.1175/1520-0442(1995)008<0784:COTSGP>2.0.CO;2

Higgins RW, Yao Y, Yarosh ES, Janowiak JE, Mo KC (1997) Influence of the Great Plains low-level jet on the summertime precipitation and moisture transport over the central United States. J Clim 10:481–507. doi:10.1175/1520-0442(1997)010<0481:IOTGPL>2.0.CO;2

Hong S-Y, Pan H-L (1998) Convective trigger function for a mass-flux cumulus parameterization scheme. Mon Weather Rev 126:2599–2620. doi:10.1175/1520-0493(1998)126<2599:CTFFAM>2.0.CO;2

Johnson DE, Tao WK, Simpson J, Sui CH (2002) A study of the response of deep tropical clouds to large-scale thermodynamic forcings. Part I: modeling strategies and simulations of TOGA COARE convective systems. J Atmos Sci 59:3492–3518. doi:10.1175/1520-0469(2002)059<3492:ASOTRO>2.0.CO;2

Kain JS, Fritsch JM (1992) The role of the convective "trigger function" in numerical forecasts of mesoscale convective systems. Meteorol Atmos Phys 49:93–106. doi:10.1007/BF01025402

Khairoutdinov MF, Randall DA (2003) Cloud resolving modeling of the ARM summer 1997 IOP: model formulation, results, uncertainties, and sensitivities. J Atmos Sci 60:607–625. doi:10.1175/1520-0469(2003)060<0607:CRMOTA>2.0.CO;2

Klemp JB, Wilhelmson RB (1978) The simulation of three-dimensional convective storm dynamics. J Atmos Sci 35:1070–1096. doi:10.1175/1520-0469(1978)035<1070:TSOTDC>2.0.CO;2

Lang S, Tao W-K, Cifelli R, Olson W, Halverson J, Rutledge S, Simpson J (2007) Improving simulations of convective systems from TRMM LBA: easterly and westerly regimes. J Atmos Sci 64:1141–1164. doi:10.1175/JAS3879.1

Lee M-I, Schubert SD (2008) Validation of the diurnal cycle in the NASA's modern era retrospective-analysis for research and applications (MERRA). In: Proceedings of the 88th AMS annual meeting, 20–24 January, New Orleans

Lee M-I, Schubert SD, Suarez MJ, Bell TL, Kim K-M (2007a) The diurnal cycle of precipitation in the NASA/NSIPP atmospheric general circulation model. J Geophys Res 112:D16111. doi:10.1029/2006JD008346

Lee M-I et al (2007b) Sensitivity to horizontal resolution in the AGCM simulations of warm season diurnal cycle of precipitation over the United States and northern Mexico. J Clim 20:1862–1881. doi:10.1175/JCLI4090.1

Lee M-I, Schubert SD, Suarez MJ, Held IM, Lau N-C, Ploshay JJ, Kumar A, Kim H-K, Schemm J-KE (2007c) An analysis of the warm season diurnal cycle over the continental United States and northern Mexico in general circulation models. J Hydrometeorol 8:344–366. doi:10.1175/JHM581.1

Lee M-I, Schubert SD, Suarez MJ, Schemm J-KE, Pan H-L, Han J, Yoo S-H (2008) Role of convection triggers in the simulation of the diurnal cycle of precipitation over the United States Great Plains in a general circulation model. J Geophys Res 113:D02111. doi:10.1029/2007JD008984

Liu C, Moncrieff MW (1998) A numerical study of the diurnal cycle of tropical oceanic convection. J Atmos Sci 55:2329–2344. doi:10.1175/1520-0469(1998)055<2329:ANSOTD>2.0.CO;2

Maddox RA (1980) Mesoscale convective complexes. Bull Am Meteorol Soc 61:1374–1387. doi:10.1175/1520-0477(1980)061<1374:MCC>2.0.CO;2

Nesbitt SW, Zipser EJ (2003) The diurnal cycle of rainfall and convective intensity according to 3 years of TRMM measurements. J Clim 16:1456–1475

Pan H-L, Wu W-S (1995) Implementing a mass flux convection parameterization package for the NMC medium–range forecast model. NMC Office Note, No. 409, p 40

Randall DA, Harsvardhan, Dazlich DA (1991) Diurnal variability of the hydrological cycle in a general circulation model. J Atmos Sci 48:40–62. doi:10.1175/1520-0469(1991)048<0040:DVOTHC>2.0.CO;2

Randall D, Khairoutdinov M, Arakawa A, Grabowski W (2003) Breaking the cloud parameterization deadlock. Bull Am Meteorol Soc 84:1547–1564. doi:10.1175/BAMS-84-11-1547

Riley GT, Landin MG, Bosart LF (1987) The diurnal variability of precipitation across the central Rockies and adjacent Great Plains. Mon Weather Rev 115:1161–1172. doi:10.1175/1520-0493(1987)115<1161:TDVOPA>2.0.CO;2

Schubert SD, Helfand HM, Wu C-Y, Min W (1998) Subseasonal variations in warm-season moisture transport and precipitation over the central and eastern United States. J Clim 11:2530–2555. doi:10.1175/1520-0442(1998)011<2530:SVIWSM>2.0.CO;2

Silva Dias PL, Bonatti JP, Kousky VE (1987) Diurnally forced tropical tropospheric circulation over South America. Mon Weather Rev 115:1465–1478. doi:10.1175/1520-0493(1987)115<1465:DFTTCO>2.0.CO;2

Soong S-T, Ogura Y (1980) Response of tradewind cumuli to large-scale processes. J Atmos Sci 37:2035–2050. doi:10.1175/1520-0469(1980)037<2035:ROTCTL>2.0.CO;2

Soong S-T, Tao W-K (1980) Response of deep tropical cumulus clouds to mesoscale processes. J Atmos Sci 37:2016–2034. doi:10.1175/1520-0469(1980)037<2016:RODTCC>2.0.CO;2

Sui CH, Lau K-M, Takayabu Y, Short D (1997) Diurnal variations in tropical oceanic cumulus convection during TOGA COARE. J Atmos Sci 54:637–655. doi:10.1175/1520-0469(1997)054<0639:DVITOC>2.0.CO;2

Sui CH, Lau K-M, Li X (1998) Convective-radiative interaction in simulated diurnal variations of tropical cumulus ensemble. J Atmos Sci 55:2345–2357. doi:10.1175/1520-0469(1998)055<2345:RCPISD>2.0.CO;2

Tao W-K, Simpson J (1989) A further study of cumulus interaction and mergers: three-dimensional simulations with trajectory analyses. J Atmos Sci 46:2974–3004. doi:10.1175/1520-0469(1989)046<2974:AFSOCI>2.0.CO;2

Tao W-K, Simpson J (1993) The Goddard cumulus ensemble model. Part I: model description. Terr Atmos Ocean Sci 4:35–72

Tao W-K, Lang S, Simpson J, Sui C-H, Ferrier B, Chou M-D (1996) Mechanisms of cloud–radiation interaction in the tropics and midlatitudes. J Atmos Sci 53:2624–2651. doi:10.1175/1520-0469(1996)053<2624:MOCRII>2.0.CO;2

Tao W-K et al (2003) Microphysics, radiation and surface processes in the Goddard cumulus ensemble (GCE) model. Meteorol Atmos Phys 82:97–137. doi:10.1007/s00703-001-0594-7

Tompkins AM (2000) The impact of dimensionality on long-term cloud-resolving model simulations. Mon Weather Rev 128:1521–1535. doi:10.1175/1520-0493(2000)128<1521:TIODOL>2.0.CO;2

Wallace JM (1975) Diurnal variations in precipitation and thunderstorm frequency over the conterminous United States. Mon Weather Rev 103:406–419. doi:10.1175/1520-0493(1975)103<0406:DVIPAT>2.0.CO;2

Webster PJ, Stephens GL (1980) Tropical upper-tropospheric extended clouds: inferences from winter MONEX. J Atmos Sci 37:1521–1541

Xie S, Zhang M (2000) Impact of the convection trigger function on single-column model simulations. J Geophys Res 105(D11): 14983–14996. doi:10.1029/2000JD900170

Xie S et al (2005) Simulations of midlatitude frontal clouds by single-column and cloud-resolving models during the Atmospheric Radiation Measurement March 2000 Cloud intensive operational period. J Geophys Res 110:D15S03. doi:10.1029/2004JD005119

Xu K-M, Randall DA (1995) Impact of interactive transfer on the macroscopic behavior of cumulus ensembles. Part II: Mechanisms for cloud–radiation interactions. J Atmos Sci 52:800–817. doi:10.1175/1520-0469(1995)052<0800:IOIRTO>2.0.CO;2

Zeng X et al (2007) Evaluating clouds in long-term cloud-resolving model simulations with observational data. J Atmos Sci 64:4153–4177. doi:10.1175/2007JAS2170.1

Zhang GJ (2003) Roles of tropospheric and boundary layer forcing in the diurnal cycle of convection in the US southern Great Plains. Geophys Res Lett 30:2281. doi:10.1029/2003GL018554

Zhang MH, Lin JL (1997) Constrained variational analysis of sounding data based on single-column integrated conservations of mass, heat, moisture, and momentum: approach and application to ARM measurements. J Atmos Sci 54:1503–1524. doi:10.1175/1520-0469(1997)054<1503:CVAOSD>2.0.CO;2

Zhang MH, Lin JL, Cederwall RT, Yio JJ, Xie SC (2001) Objective analysis of ARM IOP data: method and sensitivity. Mon Weather Rev 129:295–311. doi:10.1175/1520-0493(2001)129<0295:OAOAID>2.0.CO;2